# DYNAMICAL CHAOS AND CRITICAL BEHAVIOR IN VLASOV SIMULATIONS OF NUCLEAR MULTIFRAGMENTATION

A. Atalmi, M. Baldo, G. F. Burgio and A. Rapisarda

CSFNSM, Dipartimento di Fisica Universitá di Catania and I. N. F. N. Sezione di Catania C.so Italia 57, I-95129 Catania, Italy

#### ABSTRACT

We discuss the presence of both dynamical chaos and signals of a second—order phase transition in numerical Vlasov simulations of nuclear multifragmentation. We find that chaoticity and criticality are strongly related and play a crucial role in the process of fragments formation. This connection is not limited to our model and seems a rather general feature.

## 1. Introduction

In the last decade the phenomenon of nuclear multifragmentation in heavy-ion reactions at intermediate energies and the possibility of observing a phase transition in nuclear matter has stimulated many experimental and theoretical investigations <sup>1,2,3,4</sup>. Very recently the publication of clear experimental evidence for a phase transition <sup>5,6,7</sup> has confirmed the first theoretical conjectures, reinforcing, on the other hand, serious and puzzling questions. Can one really speak of a phase transition in a finite and transient system? Are we facing a transition of a kind already known? What is the role of the long-range Coulomb forces? Is it a 1st or 2nd order phase transition? Can we distinguish between the two in a finite system? Is statistical equilibrium reached? What is the role of dynamical chaos? In the effort to answer to the above questions a variety of dynamical and statistical models have been proposed in the past<sup>3,4,8,9,10</sup>. Two main scenarios seem to emerge from what we know at the moment. At incident energies of 50-100 MeV/A and for central collisions collective flow and dynamical effects seems to play a major role. In this case, one expects that some memory of the most important collective excited modes should remain <sup>11,12</sup>. On the other hand, at higher energies and for peripheral collisions, collective flow should become less important and thermal equilibrium is very likely reached<sup>5,6</sup>. In both cases, it seems that the hot system formed in the first stage of the reaction expands and enters the spinodal region of nuclear matter in the cooling phase. It is at this moment that the process of fragment formation begins. In the first scenario the time

scale is very fast  $\sim 50 \ fm/c$ , while, in the other one, one has to wait  $\sim 150-200 \ fm/c$ before fragments appears. Prompt statistical models seem to describe quite well this second scenario where some kind of thermalization is reached <sup>3,4</sup>. In the following we will consider only this kind of multifragmentation. The break-up of the hot composite system into several big fragments with  $Z \geq 3$  is however a very rapid process. At the same time, it is also different from standard statistical phenomena like fission or compound nucleus formation, whose typical time-scale is of the order of thousands fm/c. It is therefore not clear why statistical models<sup>3,4</sup> are able to explain the experimental data. On the other hand, their undoubted success indicates that the phase space dominates the population of the final channels. In such a fast process, the tendency of filling uniformly the phase space cannot occur in each collisional event. The system has not enough time to explore, during the reaction, the whole phase space, as can happen for compound nucleus collisions. It can be expected, therefore, that the reaction dynamics is dominated by the phase space only when the physical quantities are averaged over large sets of events. This assumption implies that the nuclear dynamics in the multifragmentation regime is irregular or chaotic enough to produce, at least approximately, a uniform "a priori" probability to populate each region of the available phase space. In particular, the formation of the final fragments must follow an irregular dynamics. This conjecture can be also inferred by the large event-to-event fluctuations observed experimentally on the charge and mass distributions. In this respect the hypothesis that multifragmentation could be reminiscent of a phase transition finds a natural explanation <sup>13,14,15,16,17</sup>. The crucial role of deterministic chaos in multifragmentation was found in Vlasov-Nordheim simulations in refs. 18,19,20 and it was recently confirmed by Classical Molecular Dynamics calculations<sup>21</sup> in connection with a critical behavior. In the following, we discuss nuclear multifragmentation along the same line of refs. 18,19 presenting the latest results. The model was first proposed in ref.<sup>9</sup> and it represents a schematic but precise and instructive guideline for understanding the dynamics of fragment formation <sup>19</sup>. After a short description of the model in section 2, we report in section 3 recent calculations<sup>20</sup>, which show how rapidly the system reaches statistical equilibrium by means of deterministic chaos. In particular scatter plots of the excited modes are studied as a function of time and fractal dimensions are calculated. In section 4, we show for the first time that, within this mean-field approach, a critical behavior can be also obtained, if an event-to-event analysis is performed. Conclusions are drawn in section 5, where we conjecture that, the strong relation between phase transitions and chaoticity found in our simulations is a rather general feature, as confirmed by several recent studies<sup>21,22,23</sup>.

#### 2. The model

The Vlasov-Nordheim equation was solved numerically in a two-dimensional lattice <sup>18,19,20</sup> using the same code of ref.<sup>9</sup>. The collision integral was actually considered only in a few simulations <sup>19</sup> not reported in this paper. Actually it seems that two-body collisions change only slightly the features here discussed. In the following we

will refer only to Vlasov simulations. We studied a fermion gas situated on a large torus with periodic boundary conditions, and its size was kept constant during the evolution. The torus sidelengths are equal to  $L_x = 51 \text{ fm}$  and  $L_y = 15 \text{ fm}$ . We divided the single particle phase space into several small cells. We employed in momentum space 51x51 small cells of size  $\Delta p_x = \Delta p_y = 40 \ MeV/c$ , while in coordinate space  $\Delta x = 0.3333$  fm and  $\Delta y = 15$  fm, i.e. we considered only one big cell on the y-direction. The initial local momentum distribution was assumed to be the one of a Fermi gas at a fixed temperature T=3~MeV. We employed a local Skyrme interaction which generates a mean field  $U[\rho] = t_0 (\rho/\rho_0) + t_3 (\rho/\rho_0)^2$ . The density  $\rho$  was folded along the x-direction with a gaussian  $e^{-x^2/\mu^2}$  with  $\mu = 0.61 fm$ , in order to give a finite range to the interaction. The parameters of the force  $t_0$  and  $t_3$  were chosen in order to reproduce correctly the binding energy of nuclear matter at zero temperature, and this gives  $t_0 = -100.3 \ MeV$  and  $t_3 = 48 \ MeV$ . The resulting EOS gives a saturation density in two dimensions equal to  $\rho_0 = 0.55 \ fm^{-2}$  which corresponds to the usual three-dimensional Fermi momentum equal to  $P_F = 260 \ MeV/c$ . The step adopted for the time evolution was equal to  $\Delta t = 0.5 \ fm/c$ . For more details concerning the model see refs.<sup>9,18,19</sup>.

## 3. Multifragmentation and Deterministic Chaos

In order to investigate the regular or irregular behavior of the mean-field dynamics with respect to multifragmentation, we studied the response of the system to small initial perturbations inside the spinodal region of nuclear matter. In our simulations we neglect the initial part of the process which drives the system inside the spinodal zone. Therefore the most realistic way to perturb our system is obtained by imposing a uniform and small white noise on the average density profile. This random initialization will mimic the initial uncertainties.

In fig.1 we show the time evolution of the density profiles for two random-initialized events started at half the saturation density. The initial perturbation was 1% of the average density. Notice the different scale used in the upper panels of the figure in order to magnify the initial noise. Though this perturbation is extremely small at t=0 and the two initializations are very close in phase space, fluctuations are amplified and distorted during the time evolution. The two simulations evolve following different deterministic paths in a complete unpredictable way. As a further evidence of this behavior, the power spectra corresponding to the density profiles are shown in fig.2. The broad range of modes  $n_k$  initially excited  $(n_k = kL_x/2\pi)$  evolve differently in each run. No particular mode is privileged by the dynamics apart from a natural cut-off of the highest modes due the finite range of the interaction. For more details see refs. <sup>18,19,20</sup>.

The above arguments give already a first qualitative idea of the sensitivity to the initial conditions and the irregularity of the following evolution which are typical features of deterministic chaos.



A way to quantify chaotic behavior is by calculating the largest Lyapunov exponent  $\lambda$ , i.e. the average rate of divergency between two close trajectories in phase space. This calculation was done in refs. <sup>18,19</sup> where a value ranging from 0.028 to 0.1 c/fm was extracted according to the initial density considered inside the spinodal region. Outside this zone, on the other hand,  $\lambda = 0$  and the dynamics is regular. Actually, due to the unbound dynamics and its limited time scale, the finite and positive value obtained for the largest Lyapunov exponent is not a unique signature of chaoticity. For a critical review of this quantity see ref.<sup>20</sup>. However, it should be noticed that, the sensitive dependence on the initial conditions shown in figs.1,2 and the positive Lyapunov exponent found, leave no room to ambiguities of any sort.

The time scale related to the chaotic behavior,  $\tau = 1/\lambda$ , is of the order of ~10-30 fm/c. If one adds to this time the transient time interval of ~ 20 fm/c needed by the largest exponent to prevail on the others, then the mean-field evolution becomes irregular and unpredictable after ~40-50 fm/c. This is in perfect agreement with what found in ref.<sup>12</sup>, where (see fig.3 of ref.<sup>12</sup>) linear response reproduces the numerical simulations only up to ~ 50 fm/c.

A further and impressive way to show the onset of chaoticity can be obtained by plotting the final amplitudes of the excited modes as a function of the initial ones. This technique has been widely used for chaotic scattering <sup>24,25</sup> and it was adopted in ref. 19 for two coupled harmonic oscillators. In fig. 3 we show these scatter plots as a function of time for 500 random-initialized events at an average density  $\rho/\rho_0 = 0.5$ . Only the modes  $n_k = 5{,}14$  are shown<sup>20</sup>. Similar plots were done independently in ref.<sup>26</sup>. The figure illustrates very clearly that after an initial linear and regular evolution, whose time scale depends on the mode considered, the onset of chaos leads to the appearance of wild fluctuations. Please notice that the numerical algorithm is under control and the total energy is conserved within 1%. The fluctuations are due only to the non-integrability of the Hamiltonian which produces this irregular evolution. In other words, the fluctuations are an intrinsic feature of the deterministic equations considered and not a spurious numerical noise. It is important to stress that the time of fragment formation  $\sim 100-150$  fm/c (see fig.1) is much longer than the time for chaos onset, therefore multifragmentation is strongly affected by this irregular evolution.

In order to quantify the dispersion of the points plotted in fig.3 one can calculate the fractal correlation dimension  $D_2$  <sup>24</sup> using the Grassberger and Procaccia correlation integral<sup>27</sup>. The latter is defined as

$$C(r) = \frac{1}{M^2} \sum_{i,j}^{M} \Theta(r - |\mathbf{z}_i - \mathbf{z}_j|) , \qquad (1)$$

 $\Theta$  being the Heaviside step function,  $\mathbf{z}_i$  a vector whose two components  $(x_i, y_i)$  are the initial and final amplitudes of the modes, M the total number of points and r a sampling interval. For small r one gets  $C(r) \sim r^{D_2}$ .  $D_2$  is the fractal correlation dimension. It has been used in nonlinear dynamics to study how often each part of a

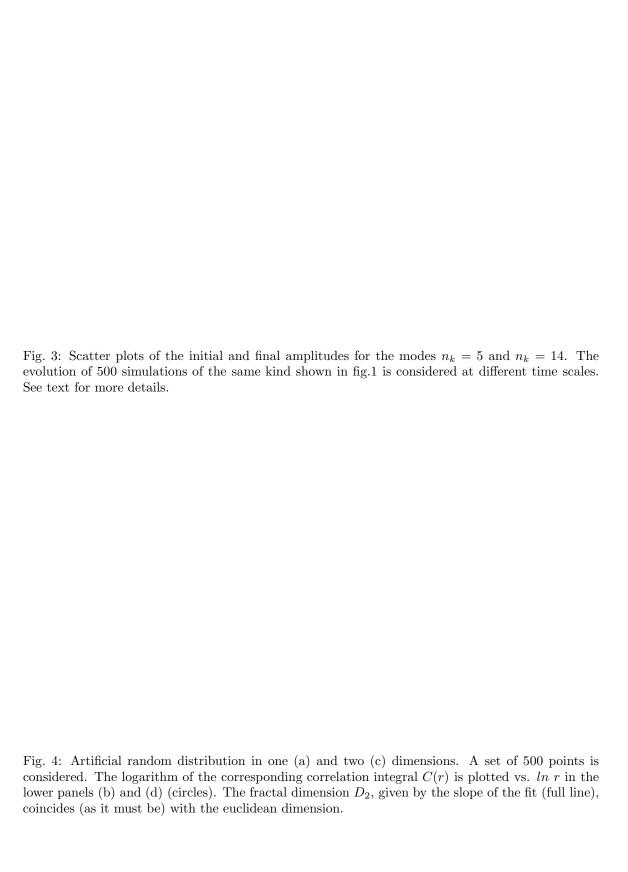


Fig. 5: The behavior of  $\ln C(r)$  vs.  $\ln r$  is plotted (circles) for the modes  $n_k = 5$  (a) and  $n_k = 14$  (b) at t=120 fm/c. The full line is the linear fit, whose slope gives the fractal dimension  $D_2$  reported. See text for more details.

strange attractor is visited. In general it gives information on how filled is the phase space. For more details see ref.<sup>24,27,28</sup>.

In fig.4 (b)(d) we display as an example the scaling behavior of  $\ln C(r)$  versus  $\ln r$  (open circles) for two sets of points distributed at random on a line (a) and on a plane (c). As expected one gets, from the slopes of the linear fits (full line), a value of  $D_2$  equal to the euclidean dimension within the errors. The latter are due to the limited number of points considered. In this case, in order to test the accuracy of the algorithm only 500 points were taken into account. So the method is reliable to calculate  $D_2$  in the case of our Vlasov scatter plots.

In fig.5 we show the scaling behavior obtained for the scatter plots of fig.3 at t=120 fm/c. The full line is the linear fit of the numerical simulation (open circles), which enables to extract the value  $D_2 = 1.96 \pm 0.05$  and  $D_2 = 1.94 \pm 0.06$  respectively. Finite size effects limit this scaling which in any case extends to several decades <sup>20</sup>. The behavior of the Vlasov calculations is very similar to that obtained for the 2D random distribution of fig.4 (c,d). This means that at t=120 fm/c for both modes we have complete randomness.

The time evolution of  $D_2$  from 1 to 2 is clearly evident in fig.6. The calculations refers to the scatter plots of fig.3. In general, while the onset of deterministic chaos starts around 40-50 fm/c for the lowest modes, the dynamics is more regular for the highest ones. However after  $\sim 80$  fm/c the evolution tends to a complete random distribution.

This result is true for all the modes excited and leaves no room for regularity of any sort. In other words there is a clear tendency towards equilibration and complete

Fig. 6: Correlation dimension  $D_2$  as a function of time for the irregular evolution of the modes  $n_k = 5$  and  $n_k = 14$  displayed in fig.3.

filling of phase-space. This is just what all the statistical models <sup>3,4</sup> assume as a starting point. Hence these schematic numerical simulations demonstrate that, even within a mean-field description, one can reach statistical equilibration in a very short time scale if the system enters the spinodal region where chaoticity is at work.

#### 4. Critical behavior

In general sharp second—order phase transitions can be observed only in macroscopic systems <sup>29,30</sup>, however also in small finite systems one can find clear signals of critical behavior <sup>13,14,31,32</sup>. In finite systems the singularities are smoothed, but one can still extract critical exponents which are very close to those of the infinite system. By using percolation<sup>13,14</sup>, classical molecular dynamics <sup>17</sup> and statistical models <sup>16</sup> it has been claimed that nuclear matter can show signals of a second—order phase transition. Some preliminary indication of criticality was observed many years ago<sup>1,34,13</sup>, but it was only very recently that critical exponents were extracted from exclusive experimental nuclear data<sup>5,7</sup>.

In general, one studies cluster size distributions by considering the conditional moments

$$M_k = \sum s^k n(s, \epsilon) \quad , \tag{2}$$

where  $n(s, \epsilon)$  is the number of fragments of size s and  $\epsilon$  is a variable which indicates the distance from the critical point. For thermal transitions  $\epsilon = T_c - T$ , while for percolation  $\epsilon = p - p_c$ ,  $T_c$  and  $p_c$  being respectively the critical temperature and the threshold probability. The summation runs over all fragments except the heaviest one. Near the critical point one gets the scaling behavior

$$n(s,\epsilon) \sim s^{-\tau} f(\epsilon s^{\sigma})$$
 , (3)

 $\tau$  and  $\sigma$  being two critical exponents. At the critical point  $\epsilon = 0$  and f(0) = 1, therefore the cluster size distribution shows a power law. Moreover the k-moments obey the scaling relation

$$M_k \sim |\epsilon|^{-(1+k-\tau)/\sigma}$$
 (4)

In particular for the first three moments one gets

$$M_0 \sim |\epsilon|^{2-\alpha}$$
 ,  $M_1 \sim (\epsilon)^{\beta}$  ,  $M_2 \sim |\epsilon|^{-\gamma}$  , (5)

where  $\alpha$ ,  $\beta$  and  $\gamma$  are characteristic critical exponents.

Critical exponents are not all independent and satisfy the relation

$$\gamma + 2\beta = 2 - \alpha = \frac{(\tau - 1)}{\sigma} \quad . \tag{6}$$

In the infinite system, at the critical point, the moments with  $k \geq 2$  diverge and also the correlation length  $\xi$  diverges as

$$\xi \sim |\epsilon|^{-\nu}$$
 , (7)

where  $\nu$  is another critical exponent related to those above discussed <sup>29,30</sup>. Therefore, at the critical point, fluctuations become very large and involve the whole system even if the microscopic forces have a very small range. The details of this microscopic interactions are not important any longer and one observes universal features. There are several classes of universality - percolation and liquid-gas are two examples. Each class has different critical exponents. We report in table 1 the value of some exponents for percolation (2D and 3D) and liquid-gas phase transition. For a more detailed discussion on critical behavior see ref.<sup>29,30,33</sup>.

In analyzing nuclear data it is difficult to identify a model-independent critical control parameter. In general one cannot define an average cluster size distribution  $n(s,\epsilon)$ . In ref.<sup>13</sup> it was shown that, in order to avoid this difficulty, an event-to-event analysis could be performed to investigate critical behavior. In particular one can define the conditional moments for each single event as

$$M_k^j = \sum s^k m^j(s) \quad , \tag{8}$$

where  $m^{j}(s)$  is the number of fragments of size s in the event j. The summation runs over all fragments, excluding the heaviest one produced in the event.

It was just by using such moments that Campi<sup>13</sup> found in the inclusive nuclear data by Waddington and Freier<sup>34</sup> clear signatures of criticality. Along the same lines the analysis was performed for statistical<sup>16</sup> and dynamical models<sup>17</sup>.

Fig. 7: The logarithm of the largest cluster size P is plotted versus the logarithm of the second moment  $M_2$  for an ensemble of 954 Vlasov simulations. Each event was generated with a random initialization as in fig.1 and inside the spinodal region. Different starting average densities - in the range  $\rho/\rho_0 = 0.4 - 0.6$  - were considered. See text for further details.

In what follows, by means of the conditional moments defined in eq.(8), we will show for the first time that it is possible to obtain signals of criticality also within Vlasov simulations of nuclear multifragmentation. This fact is important since, in our case, criticality is induced by chaotic dynamics.

In ref. 19 it was already discussed the fact that in our Vlasov numerical simulations of nuclear multifragmentation deterministic chaos produces broad cluster size distributions and strong event-to-event fluctuations so typical of multifragmentation data. In particular a power law behavior was found with an exponent  $\tau \sim 2.17 \pm 0.3$ . In that case the amount of events considered was very small,  $\sim 100$ , and one could not go beyond that. In the following, investigating a larger ensemble consisting of 954 random-initialized multifragmentation events started inside the spinodal region, we will present some preliminary results which show unambiguous signals of critical behavior. More precisely, as previously discussed, we perturbed our system with a small white noise inside the spinodal region. Several initial average densities ranging from 0.4 to  $0.6 \rho/\rho_0$  were taken into account. Then we followed the Vlasov time evolution as in fig.1 until well defined clusters were formed. The time scale to get final fragments ranges from  $\sim 300$  fm/c for  $\rho/\rho_0 = 0.6$  to  $\sim 80$  fm/c for  $\rho/\rho_0 = 0.4$ . The size of the fragments was taken along the x-direction, considering all those neighbouring cells whose density was bigger than the freeze-out one. We considered as freeze-out density the value  $\rho_{freeze-out} = 0.1 \ fm^{-2}$ , which corresponds to  $\sim 20\% \ \rho_0$ . We have checked that small variations of the freeze-out density do not produce significant changes<sup>19</sup>.

In fig. 7 we plot the logarithm of the size of largest fragment P versus the logarithm

Fig. 8: We plot  $\ln P$  versus  $\ln < M_2 >$  for the same ensemble of the previous figure (open circles). The full lines are linear fits of the two branches. The slopes of the fits give the ratio of the critical exponents  $\beta/\gamma$ . More precisely the upper (subcritical) one gives  $-\beta/\gamma = -0.27 \pm 0.1$ , while the lower (overcritical) one gives  $1 + \beta/\gamma = 1.46 \pm 0.1$ .

of the second moment  $M_2$ . The figure shows a typical critical triangular pattern with a subcritical upper branch and an overcritical lower one. 'Evaporation-like' events in the upper branch are obtained for initial densities  $\rho/\rho_0 \sim 0.6$ , whereas 'vaporization-like' events are found for  $\rho/\rho_0 \sim 0.4$ . Critical events are mostly in the range  $\rho/\rho_0 \sim 0.55 - 0.5$ . In general large fluctuations exist from event to event. The two branches meet at the critical point. Similar plots were also obtained in refs.<sup>13</sup> for cubic bond percolation model with a number of sites  $A = 6^3$  and the gold multifragmentation emulsion data by Waddington and Freier<sup>34</sup>.

The indication given by fig.7 is important but qualitative. One should extract crit-

exponent	β	$\gamma$	$\beta/\gamma$	au
$2D \ Percolation^{33}$	0.14	2.4	0.058	2.0
3D Percolation <sup>33</sup>	0.41	1.8	0.23	2.18
$Liquid - gas^{29}$	0.33	1.23	0.27	2.21
Emulsion data <sup>13</sup>	-	-	$0.2 \pm 0.1$	$2.17 \pm 0.1$
EOS data <sup>5</sup>	$0.29 \pm 0.02$	$1.4 \pm 0.1$	$0.21 \pm 0.1$	$2.14 \pm 0.06$
Vlasov	-	-	$0.37 \pm 0.2$	$2.27 \pm 0.2$

Table 1: Comparison of Vlasov critical exponents with those of percolation (2D and 3D), liquid-gas and experimental nuclear data.

ical exponents to have a quantitative information. Following the procedure adopted in ref.<sup>16</sup> we took the average of  $M_2$  at a fixed size of the largest cluster P. In this way one can try to extract the slopes of the two branches which should give the ratio between the critical exponents  $\beta$  and  $\gamma$ . In fact the lower branch should have a slope given by  $1+\beta/\gamma$ , while the upper branch  $-\beta/\gamma^{13,16}$ . In fig.8 we plot  $\ln P$  as a function of the logarithm of the average  $< M_2 >$  (open circles). In the figure are shown also the linear fits (full lines) of the two branches and the values of the slopes obtained. The statistics of the upper branch is poorer than that of the lower branch - as can be seen in fig.7. For this reason the first point of the upper branch was excluded from the fit. From the two slopes one gets consistent values within the errors, i.e.  $-\beta/\gamma = -0.27 \pm 0.1$  and  $1 + \beta/\gamma = 1.46 \pm 0.1$  Taking an average between the two values one finds  $\beta/\gamma = 0.37 \pm 0.2$ . The ratio between  $\beta$  and  $\gamma$  can be used to extract the value of  $\tau$ . In fact from eqs.(4-6) one obtains the relation

$$\tau = \frac{2 + 3\beta/\gamma}{1 + \beta/\gamma} \quad . \tag{9}$$

From the above equation and our estimate of  $\beta/\gamma = 0.37 \pm 0.2$  we get  $\tau = 2.27 \pm 0.2$ , which is consistent to what previously obtained<sup>19</sup>.

It is important to stress at this point, that we start our system inside the spinodal region, thus it is not clear at the moment what kind of phase transition the system is reminiscent of. We find signals of criticality in the sense that the instabilities of the spinodal zone, driven by deterministic chaos, produce inclusive cluster size distributions of different shapes, as in percolation or liquid-gas phase transitions, according to the initial average density adopted. At variance with percolation, which is a geometric model, we have a nuclear-like dynamics. It is not clear what are the links, if any, between this behavior and the standard liquid-gas phase transition. The system in fact should not be close to the critical point<sup>19</sup>. A deeper understanding of this kind of criticality is beyond the aim of the present paper and is left for the future<sup>35</sup>.

In table 1 we report the value of the critical exponents  $\beta$ ,  $\gamma$  and  $\tau$  obtained in our calculations together with those of percolation (in 2D and 3D) and the liquid-gas case. The values of the Waddington<sup>13</sup> and EOS data<sup>5</sup> are also shown for comparison. In general the values we get from our Vlasov simulations are not so different from the 3D percolation and the liquid-gas phase transition. However, before drawing definite conclusions some comments must be done. i) The numerical calculation of critical exponents is a very delicate problem and our present analysis is rather crude. ii) The statistics we used is rather poor, expecially for subcritical events. iii) We have no idea of the absolute values of  $\beta$  and  $\gamma$ . iv) Our simulations are in 2 dimensions and the cluster sizes were considered only along the x-coordinate.

On the other hand, it is very remarkable that a schematic model like ours is able to give such a critical behavior. Please notice also the close similarity of our values with those extracted from the available experimental data. This fact deserves a further comment since we neglected the coulomb force. In fact, according to statistical calculations<sup>16</sup>, the coulomb force can strongly influence the critical exponents. However no evidence of this influence seems to be present in the available experimental data. A further puzzling question is the understanding of the link between this critical behavior and liquid-gas transition.

As a general statement, we can say that the above discussed results though very impressing and stimulating pose many troubling questions and leave several open problems. A more severe analysis in order to clarify the situation is in progress<sup>35</sup>.

#### 5. Conclusions

In this paper we concisely reviewed recent numerical simulations of nuclear multifragmentation. The growth of density fluctuations, in the spinodal region of nuclear matter EOS, has been advocated as the mechanism of fragment formation. We studied the dynamics of such a process by solving the Vlasov equation numerically on a lattice. The nuclear system in the spinodal region was schematized by a twodimensional fluid confined inside a fixed torus. The initially homogeneous system was perturbed by adding a small and random density fluctuation. This was done in order to simulate the initial uncertainties produced by the missing initial dynamics. The time evolution was then followed up to the time of fragment formation, when several well separated density humps appear. The study of scatter plots of the excited modes confirmed the chaotic character of the dynamics found already in refs. 18,19. In the present contribution it was shown that chaos is strong enough to fill uniformly the available phase space. This fact was quantified by the calculation of the fractal correlation dimension  $D_2$ . Chaos is fully developed in a short and limited time interval, of the order of 80-120 fm/ $c^{20}$ . In this respect such a chaotic dynamics is a transient phenomenon similar to the case of chaotic scattering<sup>25</sup>.

These results give a strong theoretical support to the statistical models<sup>3,4</sup> successfully used in analyzing most of the available nuclear multifragmentation data.

Finally, using an ensemble of 954 Vlasov simulations started inside the spinodal region, an event-to-event analysis of the cluster size distributions was performed along the same lines of refs.<sup>13,16</sup>. Unambiguous signals of critical behavior were found also in our case. The extracted ratio of the critical exponents  $\beta/\gamma$  and of  $\tau$  are in agreement with those of liquid-gas, 3D percolation and the available experimental data<sup>13,34,5</sup>. At the moment both the analysis and the model are too schematic to discriminate among different universality classes or to draw final conclusions. Here we do not want to stress too much the values of the critical exponents obtained, but it seems very important that both chaoticity and criticality are found in the process of multifragmentation. Very recently a similar coexistence was found also in other models<sup>21,22,23</sup>. This fact confirms the general character of this feature, which could probably be explained by the enhancement of phase-space volume and entropy during the phase transition. Chaoticity is probably another indication of phase transition. Such an appealing

general perspective is at the moment only a sound conjecture which needs further investigation.

### 6. Acknowledgments

We would like to thank M. Belkacem, A. Bonasera and V. Latora for several stimulating discussions.

## 7. References

- [1] J.E. Finn et al. Phys. Rev. Lett. 49 (1982) 1321.
- [2] G.F. Bertsch and P.J. Siemens, *Phys. Lett.* B **126** (1984) 9.
- [3] D.H.E. Gross, *Prog. Part. Nucl. Phys.* **30** (1993) 155 and refs. therein.
- [4] J.P. Bondorf, A.S. Botvina, A.S. Iljinov, I.N. Mishustin and K. Sneppen, *Phys. Rep.* **257** (1995) 133 and refs. therein.
- [5] M.L. Gilkes et al. Phys. Rev. Lett. **73**(1994) 1590.
- [6] J. Pochodzalla et al. Phys. Rev. Lett. 75 (1995) 1040, G.J. Kunde et al. Phys. Rev. Lett. 74 (1995) 38 and also M. Begemann-Blaich's contribution to this conference.
- [7] A. Wörner Ph.D. thesis (1995), unpublished.
- [8] G.F. Bertsch and S. Das Gupta, Phys. Rep. 160 (1988) 189.
- [9] G.F. Burgio, Ph. Chomaz and J. Randrup, Phys. Rev. Lett. 69 (1992) 885.
- [10] L. Moretto, K. Tso, N. Colonna, G. Wozniak , Phys. Rev. Lett. 69 (1992) 1884;
  W. Bauer, G. Bertsch and H. Schultz, Phys. Rev. Lett. 69 (1992) 1888.
- [11] M. Colonna, M. Di Toro and A. Guarnera Nucl. Phys. A 580, (1994) 312.
- [12] B. Jacquot, M. Colonna, Ph. Chomaz and A. Guarnera *Phys. Lett.* **B** 359, (1995) 268; see also A. Guarnera's contribution to this conference.
- [13] X. Campi, J. of Phys. A19 (1986) 917; Phys. Lett. B 208 (1988) 351; J. de Phys. 50 (1989) 183.
- [14] W. Bauer, *Phys. Rev.* C38 (1988) 1297;
- [15] M. Ploszajczak and A. Tucholski, Phys. Rev. Lett. 65 (1990) 1539; P. Bozek,
  M. Ploszajczak and R. Botet, Phys. Rep. 252 (1995) 101.
- [16] H.R. Jaqaman and D.H.E. Gross, Nucl. Phys. A 524 (1991) 321.
- [17] V. Latora, M. Belkacem and A. Bonasera, Phys. Rev. Lett. 73 (1994) 1765; M. Belkacem, V. Latora and A. Bonasera, Phys. Rev. C 52 (1995) 271; see also Belkacem's contribution to this conference.
- [18] G.F. Burgio, M. Baldo and A. Rapisarda, Phys. Lett. B 321 (1994) 307; M. Baldo, G.F. Burgio and A. Rapisarda, Nucl. Phys. A583 (1995) 343.
- [19] M. Baldo, G.F. Burgio and A. Rapisarda, Phys. Rev. C 51 (1995) 198.
- [20] A.Atalmi, M. Baldo, G.F. Burgio and A. Rapisarda, Univ. of Catania pp.n.95-08, *Phys. Rev.* C in press.
- [21] A. Bonasera, V. Latora and A. Rapisarda, Phys. Rev. Lett. 75 (1995) 3434.
- [22] S.K. Nayak, R. Ramaswamy and C. Chakravarty *Phys. Rev.* **E 51** (1995) 3376.

- [23] Y. Yamaguchi, preprint DPNU-96-06, chao-dyn/9602002.
- [24] E. Ott, Chaos in Dynamical Systems, Cambridge University Press 1993;
- [25] A. Rapisarda and M. Baldo, Phys. Rev. Lett. 66 (1991) 2581; M. Baldo, E.G. Lanza and A. Rapisarda, Chaos 3 (1993) 691.
- [26] B. Jacquot, A. Guarnera, Ph. Chomaz and M. Colonna, GANIL preprint P95-17, Phys. Rev. C submitted.
- [27] P. Grassberger and I.Procaccia, Phys. Rev. Lett. 50, (1983) 346.
- [28] G. Paladin and A. Vulpiani Phys. Rep. 156, (1987) 147.
- [29] H.E. Stanley, *Introduction to Phase Transitions and Critical Phenomena*, Clarendon Press, Oxford 1971.
- [30] J.J. Binney, N.J. Dowrick, A.J. Fisher and M.E.J. Newman, *The Theory of Critical Phenomena*, Oxford Science Publications, 1993.
- [31] J.B. Elliot et al. Phys. Rev. C 49 (1994) 3185.
- [32] W.F.J. Müller, proceedings of the XXXIII international winter meeting Bormio (Italy) 1995, ed. I. Iori, p.394.
- [33] D. Stauffer, Phys. Rep. **54** (1979) 1.
- [34] C.J. Waddington and P.S. Freier, Phys. Rev. C 31 (1985) 888.
- [35] A.Atalmi, M. Baldo, G.F. Burgio and A. Rapisarda, in preparation.

This figure "fig1-1.png" is available in "png" format from:

This figure "fig1-2.png" is available in "png" format from:

This figure "fig1-3.png" is available in "png" format from:

This figure "fig1-4.png" is available in "png" format from: